

Published in final edited form as:

*Surgery*. 2013 January ; 153(1): 52–62. doi:10.1016/j.surg.2012.04.002.

## Heparin-binding epidermal growth factor-like growth factor improves intestinal barrier function and reduces mortality in a murine model of peritonitis

Jixin Yang, MD, Andrei Radulescu, MD, PhD, Chun-Liang Chen, PhD, Hong-Yi Zhang, MD, Iyore O. James, MD, and Gail E. Besner, MD

Department of Pediatric Surgery, Nationwide Children's Hospital, Center for Perinatal Research, The Research Institute at Nationwide Children's Hospital, and The Ohio State University College of Medicine, Columbus, OH

### Abstract

**Background**—The morbidity and mortality associated with bacterial peritonitis remain high. Heparin-binding epidermal growth factor (EGF)-like growth factor (HB-EGF) is a potent intestinal cytoprotective agent. The aim of this study was to evaluate the effect of HB-EGF in a model of murine peritonitis.

**Methods**—HB-EGF<sup>(-/-)</sup> knockout (KO) mice and their HB-EGF<sup>(+/+)</sup> wild-type (WT) counterparts were subjected to sham operation, cecal ligation and puncture (CLP), or CLP with HB-EGF treatment (800 µg/kg IP daily). Villous length, intestinal permeability, intestinal epithelial cell (IEC) apoptosis, bacterial load in peritoneal fluid (PF) and mesenteric lymph nodes (MLN), inflammatory cytokine levels, and survival were determined.

**Results**—After exposure to CLP, HB-EGF KO mice had significantly shorter villi ( $1.37 \pm 0.13$  vs  $1.96 \pm 0.4$  relative units;  $P < .03$ ), increased intestinal permeability ( $17.01 \pm 5.18$  vs  $11.50 \pm 4.67$  nL/min/cm<sup>2</sup>;  $P < .03$ ), increased IEC apoptotic indices ( $0.0093 \pm 0.0033$  vs  $0.0016 \pm 0.0014$ ;  $P < .01$ ), and increased bacterial counts in PF ( $25,313 \pm 17,558$  vs  $11,955 \pm 6,653$  colony forming units [CFU]/mL;  $P < .05$ ) and MLN ( $19,009 \pm 11,200$  vs  $5,948 \pm 2,988$  CFU/mL/g;  $P < .01$ ) compared with WT mice. Administration of HB-EGF to WT and HB-EGF KO mice exposed to CLP led to significantly increased villous length and decreased intestinal permeability, IEC apoptosis and bacterial counts in MLN ( $P < .05$ ). Survival of HB-EGF KO mice subjected to CLP was significantly improved with administration of HB-EGF ( $P < .05$ ).

**Conclusion**—HB-EGF gene KO increases susceptibility to peritonitis-induced intestinal injury, which can be reversed by administration of HB-EGF. These results support a protective role of HB-EGF in peritonitis-induced sepsis.

Sepsis is a common and frequently fatal condition that kills >200,000 people each year in the United States.<sup>1</sup> The intestine plays a central role in the pathophysiology of sepsis, where it has been characterized as the “motor” of the systemic inflammatory response syndrome.<sup>2–4</sup> Perturbations to the intestinal epithelium in sepsis result in barrier dysfunction,<sup>5,6</sup> increased apoptosis,<sup>7–9</sup> and the production of cytokines,<sup>10</sup> which may result in distant organ damage leading to multiple organ failure. A number of studies have demonstrated that the loss of gut barrier function after various adverse circulatory conditions results in subsequent bacterial translocation from the intestinal lumen,<sup>11–14</sup> which

contributes to the development or exacerbation of systemic infection by allowing distant spreading of bacteria and bacterial toxins.<sup>15</sup>

Heparin-binding epidermal growth factor (EGF)-like growth factor (HB-EGF) was initially identified in the conditioned medium of cultured human macrophages<sup>16</sup> and later found to be a member of the EGF family.<sup>17</sup> Like other family members, HB-EGF binds to the EGF receptor (EGFR; ErbB-1), inducing its phosphorylation. Unlike most EGF family members, HB-EGF has the ability to bind strongly to heparin. Cell-surface heparin- sulfate proteoglycans can act as highly abundant, low-affinity receptors for HB-EGF. HB-EGF is an immediate early gene that plays a pivotal role in mediating the earliest cellular responses to proliferative stimuli and cellular injury.<sup>18</sup> Previous studies from our laboratory and from other laboratories have shown that expression of endogenous HB-EGF is significantly increased in response to tissue damage,<sup>19,20</sup> hypoxia,<sup>21</sup> and oxidative stress,<sup>22</sup> as well as during wound healing and regeneration.<sup>23</sup>

We have accumulated multiple lines of evidence supporting a role for HB-EGF in protection of the intestines from a variety of insults including intestinal ischemia/reperfusion (I/R) injury,<sup>20</sup> hemorrhagic shock and resuscitation (HS/R),<sup>24</sup> and necrotizing enterocolitis (NEC).<sup>25</sup> We have previously shown that HB-EGF knockout (KO) mice have increased intestinal injury upon exposure to intestinal I/R,<sup>26</sup> HS/R,<sup>27</sup> and NEC,<sup>28</sup> and that HB-EGF transgenic mice have decreased intestinal injury upon exposure to HS/R<sup>29</sup> and NEC.<sup>30</sup> Furthermore, we have shown that administration of exogenous HB-EGF under experimental conditions protects the intestines from intestinal I/R,<sup>31</sup> HS/R,<sup>24</sup> and NEC,<sup>25,32,33</sup> and protects the lungs from remote organ injury after intestinal I/R.<sup>34</sup> The aim of the current study was to investigate the role of HB-EGF in a completely different animal model of peritonitis-induced intestinal injury and sepsis---the model of cecal ligation and puncture (CLP), which is initiated by bacterial invasion followed by multiple organ dysfunction.

## MATERIALS AND METHODS

### Animals

Ten- to 12-week old (25–30 g) male HB-EGF<sup>(-/-)</sup> KO mice and their HB-EGF<sup>(+/+)</sup> wild-type (WT) counterparts were subjected to CLP or sham operation. HB-EGF KO mice on a C57BL/6J × 129 background and their HB-EGF WT C57BL/6J × 129 counterparts were kindly provided by Dr. David Lee (Chapel Hill, NC).<sup>35</sup> In HB-EGF KO mice, HB-EGF exons 1 and 2 were replaced with PGK-Neo, thus deleting the signal peptide and propeptide domains. The desired targeting events were verified by Southern blots of genomic DNA and exon-specific polymerase chain reaction, with Northern blots confirming the absence of the respective transcripts.<sup>35</sup> All animal protocols were approved by the Institutional Animal Care and Use Committee of the Research Institute at Nationwide Children's Hospital (Protocol # AR0800088).

### Peritonitis model

Mice were subjected to CLP according to the methodology of Baker et al<sup>36</sup> Mice were anesthetized with 2.5% isoflurane, and a 1-cm ventral midline abdominal incision was made aseptically through the skin and linea alba. The cecum was located, exteriorized, and ligated with 3-0 silk just distal to the ileocecal valve by a technique that did not result in intestinal obstruction, and was then punctured through-and-through twice with a 23-gauge needle. The cecum was then gently squeezed to extrude a small amount of stool and replaced into the abdomen, which was then closed in layers. Sham mice were treated identically, except that the cecum was neither ligated nor punctured. Animals were

humanely killed at either 24 hours for functional studies or at 7 days in survival experiments. The operators were blinded to the treatment groups.

### Administration of HB-EGF

One hour before CLP, a cohort of HB-EGF KO or WT mice received an intraperitoneal (IP) injection of HB-EGF (800 µg/kg) diluted in 1 mL of sterile phosphate-buffered saline (PBS), with control mice receiving vehicle only. For survival experiments, mice received IP injections of HB-EGF or vehicle once daily until they either died or were humanely killed at 7 days. The dosage of HB-EGF was based on our previously published work showing efficacy of HB-EGF at this dosage.<sup>25–28,32,33</sup>

### Morphologic analyses

Villus length was determined in hematoxylin and eosin (H&E) stained jejunal sections by measuring the distance from the crypt neck to the villus tip using Image J software (National Institutes of Health, Bethesda, MD). A minimum of 10 villi from each section were measured by a blinded examiner. Results were expressed in relative units, as determined by the centimeter to pixel ratio.

### Intestinal permeability

Intestinal mucosal barrier function was assessed using the ex vivo isolated everted gut sac method as described, with some modifications.<sup>37</sup> Briefly, 6-cm-long distal ileal everted gut sacs were prepared in ice-cold modified Krebs-Henseleit bicarbonate buffer (KHBB; pH, 7.4; 10 mmol/L HEPES/137 mmol/L NaCl/5.5 mmol/L KCl/4.2 mmol/L NaHCO<sub>3</sub>/0.3 mmol/L Na<sub>2</sub>HPO<sub>4</sub>/0.4 mmol/L KH<sub>2</sub>PO<sub>4</sub>/0.4 mmol/L MgSO<sub>4</sub>/0.5 mmol/L MgCl<sub>2</sub>/1.3 mmol/L CaCl<sub>2</sub>/19.5 mmol/L glucose). Fluorescein-isothiocyanate dextran (Mr 4000 Da; FD4) was used as a permeability probe. The everted gut sacs were gently distended by injecting 0.4 mL of KHBB and suspending the sacs in a 50-mL beaker containing 40 mL of KHBB with added FD4 (100 µg/mL) for 30 minutes. The incubation medium in the beaker was maintained at a temperature of 37°C and was continuously bubbled with a gas mixture containing 95% O<sub>2</sub> and 5% CO<sub>2</sub>. A 1-mL sample was taken from the beaker at the beginning of the incubation to determine the initial FD4 concentration of the mucosal side. After the 30 minutes of incubation, the fluid was aspirated from the inside of the sac to determine the FD4 concentration of the serosal side. The length and diameter of each gut sac was measured. Serosal and mucosal samples were centrifuged for 10 minutes at 1,000 × *g* at 4°C. Fluorescence of 100 µL of supernatant was measured using an LS-50 fluorescence spectrophotometer (Perkin-Elmer, Palo Alto, CA) at an excitation wavelength of 492 nm (slit width, 2.5 nm) and an emission wavelength of 515 nm (slit width, 10 nm). Gut permeability was expressed as the mucosal-to-serosal clearance of FD4 as follows<sup>27,37</sup>:

$$\text{FD4 clearance (nL/min/cm}^2\text{)} = \text{FD4}_{\text{ser}} \times (\text{Original 0.4ml} + \text{Absorbed Volume})30^{-1} \times \text{FD4}_{\text{muc}}^{-1} \times (\pi\text{DL})^{-1}$$

### Intestinal epithelial cell apoptosis

Apoptotic cells in the intestine were identified by terminal deoxynucleotidyl transferase dUTP nick-end labeling using an ApopTag Red in situ apoptosis detection kit (Chemicon International, Temecula, CA) following the manufacturer's protocol as follows. Paraffin-embedded tissue sections were deparaffinized and pretreated with freshly diluted protein digesting enzyme for 15 minutes at room temperature (RT). We applied 75 µL/5 cm<sup>2</sup> equilibration buffer directly to tissue sections and incubated for 10 seconds at RT. Excess liquid was gently tapped off the tissue sections and a working strength of Tdt enzyme (55 µL/5 cm<sup>2</sup>) was applied to the sections and allowed to incubate in a humidified chamber at 37°C for 1 hour. Slides were washed 3 times with 1 × PBS and incubated with anti-

digoxigenin conjugate for 30 minutes at RT in a dark room. Slides were washed 4 times with  $1 \times$  PBS for 2 minutes at RT and counterstained with a mounting media containing DAPI (Invitrogen, Eugene, OR). Positively stained apoptotic cells in the intestine were counted randomly in three  $40\times$  view fields for each animal in a blinded fashion. In each section, positively stained enterocytes and total enterocytes were counted using Image Pro Plus 6.2.1 for Windows (Media Cybernetics, Inc, Bethesda, MD). The apoptotic index was defined as the percent of positively stained enterocytes per 100 enterocytes.

### **Bacterial cultures of peritoneal fluid**

Twenty-four hours after CLP or sham operation, the peritoneal cavity was lavaged with 3 mL of sterile PBS to obtain peritoneal fluid (PF). Aliquots of 0.1 mL were plated in duplicate onto MacConkey agar plates (BD, Franklin Lakes, NJ) for culture of total Gram-negative bacilli. The plates were incubated for 24 hours at  $37^{\circ}\text{C}$  and then counted for bacterial colony-forming units (CFU). Results were expressed as CFU/mL  $\pm$  SD.

### **Bacterial cultures of mesenteric lymph nodes**

Twenty-four hours after CLP or sham operation, mesenteric lymph nodes (MLN) were harvested under sterile conditions and assessed for translocation of endogenous enteric bacteria. After rinsing in sterile PBS (5 mL) 3 times, MLN were weighed, homogenized in 1 mL of PBS, and aliquots of 0.1 mL were plated in duplicate onto MacConkey agar plates (BD, Franklin Lakes, NJ) for culture of total Gram-negative bacilli. The plates were incubated for 24 hours at  $37^{\circ}\text{C}$  and then counted for CFU. Results were expressed as CFU/mL  $\pm$  SD.

### **Local and systemic cytokine levels**

PF was collected as described. Blood was collected from the abdominal aorta by direct puncture. Cytokine levels of interleukin (IL)-6, IL-10, IL-12p70, monocyte chemoattractant protein-1, interferon- $\gamma$ , and tumor necrosis factor (TNF) in PF and serum were determined using a cytometric bead array (BD Mouse Inflammation Kit, San Jose, CA) according to the manufacturer's protocol. All samples were run in duplicate.

### **Animal survival study**

Additional HB-EGF KO mice and their WT counterparts were subjected to either CLP, CLP with administration of HB-EGF, or sham operation ( $n = 11$  per group). Animal survival was determined over a 7-day time period. Animals were monitored every 6 hours until the end of the 1-week study period. Mice were humanely killed upon the development of set end point criteria (abdominal distention, respiratory distress, or lethargy). All remaining animals were humanely killed at the end of experiment at 7 days.

### **Statistical analyses**

The unpaired, 2-tailed Student  $t$  test was used to compare mice subjected to CLP and mice subjected to CLP with HB-EGF treatment, and to compare the KO mice and their WT counterparts. Multiple comparisons were performed using 1-way analysis of variance. Statistical analysis was performed using Microsoft Office Excel, version 2007 for Windows (Microsoft, Redmond, WA). Survival was assessed by the Log-Rank or Fleming-Harrington test using SAS 9.1.3 (SAS Institute Inc, Cary, NC). Bacterial culture results were analyzed using the hierarchical linear model, HLM 6, SAS 9.1.3 (SAS Institute Inc). Results were expressed as mean values  $\pm$  SD.

## RESULTS

### Decreased villous length after CLP is exacerbated in HB-EGF KO mice

Villus length was assessed in H&E-stained jejunal sections from WT and HB-EGF KO mice subjected to either sham operation, CLP, or CLP with HB-EGF administration (Fig 1). WT mice subjected to CLP had significantly decreased villous length compared with WT mice subjected to sham operation ( $2.10 \pm 0.35$  vs  $2.55 \pm 0.21$  relative units;  $P = .04$ ). HB-EGF KO mice subjected to CLP had significantly decreased villous length compared with HB-EGF KO mice subjected to sham operation ( $1.37 \pm 0.13$  vs  $2.09 \pm 0.17$  relative units;  $P = .0002$ ). HB-EGF KO mice had decreased villous length compared with WT mice after sham operation ( $2.09 \pm 0.17$  vs  $2.55 \pm 0.21$  relative units;  $P = .0099$ ) and after CLP ( $1.37 \pm 0.13$  vs  $2.10 \pm 0.35$  relative units;  $P = .0034$ ). After treatment with HB-EGF, villous length increased significantly in both WT mice ( $2.65 \pm 0.33$  vs  $2.10 \pm 0.35$  relative units;  $P = .0395$ ) and KO mice ( $1.66 \pm 0.18$  vs  $1.37 \pm 0.13$  relative units;  $P = .0209$ ) subjected to CLP.

### HB-EGF KO mice have worsened intestinal permeability after CLP

We next examined intestinal permeability as a measure of gut barrier function in WT and HB-EGF KO mice exposed to sham operation, CLP, or CLP with HB-EGF administration (Fig 2). WT mice subjected to CLP had significantly increased intestinal permeability compared with WT mice subjected to sham operation ( $18.04 \pm 7.17$  vs  $6.06 \pm 2.50$  nL/min/cm<sup>2</sup>;  $P = .0254$ ). HB-EGF KO mice subjected to CLP had significantly increased intestinal permeability compared with HB-EGF KO mice subjected to sham operations ( $31.49 \pm 7.39$  vs  $13.47 \pm 2.59$  nL/min/cm<sup>2</sup>;  $P = .0237$ ). HB-EGF KO mice had significantly increased intestinal permeability under basal (non-injury) conditions compared with WT mice ( $13.47 \pm 2.59$  vs  $6.06 \pm 2.50$  nL/min/cm<sup>2</sup>;  $P = .0490$ ), as we have previously reported.<sup>28</sup> HB-EGF KO mice subjected to CLP had significantly increased intestinal permeability compared with WT mice subjected to CLP ( $31.49 \pm 7.39$  vs  $18.04 \pm 7.17$  nL/min/cm<sup>2</sup>;  $P = .0101$ ). When WT mice subjected to CLP were treated with HB-EGF, intestinal permeability was significantly improved ( $11.98 \pm 3.25$  vs  $18.04 \pm 7.17$  nL/min/cm<sup>2</sup>;  $P = .0393$ ). When HB-EGF KO mice were subjected to CLP but treated with HB-EGF, intestinal permeability was also significantly improved ( $18.15 \pm 6.64$  vs  $31.49 \pm 7.39$  nL/min/cm<sup>2</sup>;  $P = .0116$ ).

### HB-EGF KO mice have increased IEC apoptosis after CLP

Because apoptosis is a major mode of intestinal epithelial cell (IEC) death induced by CLP, we next evaluated IEC apoptosis in our model. WT mice subjected to CLP had increased IEC apoptosis compared with WT mice subjected to sham operations ( $0.0141 \pm 0.0189$  vs  $0.0008 \pm 0.0003$  mean apoptosis index;  $P = .082$ ; Fig 3). WT mice subjected to CLP but treated with HB-EGF had decreased apoptosis compared with WT mice subjected to CLP only ( $0.0024 \pm 0.0028$  vs  $0.0141 \pm 0.0189$  mean apoptosis index;  $P = .092$ ). HB-EGF KO mice subjected to CLP had increased IEC apoptosis compared with HB-EGF KO mice subjected to sham operation, and this reached statistical significance ( $0.0541 \pm 0.0554$  vs  $0.0009 \pm 0.0004$  mean apoptosis index;  $P < .05$ ). HB-EGF KO mice subjected to CLP had increased IEC apoptosis compared with WT mice subjected to CLP ( $0.0541 \pm 0.0554$  vs  $0.014 \pm 0.019$  mean apoptosis index;  $P < .05$ ). HB-EGF KO mice subjected to CLP but treated with HB-EGF had significantly decreased IEC apoptosis compared with HB-EGF KO mice subjected to CLP only ( $0.0541 \pm 0.0554$  vs  $0.0035 \pm 0.0016$  mean apoptosis index;  $P < .05$ ).

### HB-EGF KO mice have increased bacterial growth in PF and MLN after CLP

WT mice subjected to CLP had significantly increased bacterial growth in PF ( $11,955 \pm 6,654$  CFU/mL) and MLN ( $5,949 \pm 2,989$  CFU/mL/g) compared with WT mice subjected to



sham operation (Fig 4). HB-EGF KO mice subjected to CLP had significantly increased bacterial growth in PF ( $25,314 \pm 17,558$  CFU/mL) and MLN ( $19,010 \pm 11,200$  CFU/mL/g) compared with HB-EGF KO mice subjected to sham operation. HB-EGF KO mice subjected to CLP had increased bacterial growth in PF ( $25,314 \pm 17,558$  CFU/mL vs  $11,955 \pm 6,653$  CFU/mL;  $P = .0327$ ) and in MLN ( $19,010 \pm 11,200$  CFU/mL/g vs  $5,949 \pm 2,989$  CFU/mL/g;  $P = .0015$ ) compared with WT mice subjected to CLP. WT mice subjected to CLP but treated with HB-EGF had significantly decreased bacterial growth in MLN ( $3,289 \pm 648$  CFU/mL/g vs  $5,949 \pm 2,989$  CFU/mL/g;  $P = .0069$ ) compared with WT mice subjected to CLP. HB-EGF KO mice subjected to CLP but treated with HB-EGF had decreased bacterial growth in PF and MLN, and this reached statistical significance in MLN ( $19,010 \pm 1,1200$  CFU/mL/g vs  $7,163 \pm 1,441$  CFU/mL/g;  $P = .0255$ ).

### Local and systemic cytokine levels

Pro- and anti-inflammatory cytokine levels were determined in both PF and serum 24 hours after CLP. The pro-inflammatory cytokines TNF- $\alpha$ , IFN- $\gamma$ , and IL-6, and the anti-inflammatory cytokine IL-10, were all significantly increased in PF and serum from WT mice subjected to CLP compared with WT mice subjected to sham operation ( $P < .01$  for each), with the exception of IFN- $\gamma$  levels in the serum which were unchanged (Fig 5). WT mice subjected to CLP but treated with HB-EGF had decreased levels of TNF- $\alpha$  ( $91.06 \pm 78.55$  pg/mL vs  $286.99 \pm 233.99$  pg/mL;  $P = .0616$ ), IFN- $\gamma$  ( $1.46 \pm 1.07$  pg/mL vs  $3.66 \pm 2.75$  pg/mL;  $P = .0616$ ), IL-6 ( $553.15 \pm 122.54$  pg/mL vs  $3,000.88 \pm 3,095.14$  pg/mL;  $P = .29$ ), and IL-10 ( $97.54 \pm 19.13$  pg/mL vs  $659.06 \pm 738.89$  pg/mL;  $P = .4334$ ) in PF compared with WT mice subjected to CLP only, although these values did not attain significance. The levels of these cytokines in PF and serum were decreased in HB-EGF KO mice subjected to CLP compared with WT mice subjected to CLP ( $P < .05$  for each), with the exception of IFN- $\gamma$  levels in the serum, which were unchanged. HB-EGF KO mice exposed to CLP had significantly increased PF and serum TNF- $\alpha$  and IL-6 compared with HB-EGF KO mice subjected to sham operation ( $P < .01$  for each). Serum levels of IL-10 were significantly increased in HB-EGF KO mice subjected to CLP that received HB-EGF compared with HB-EGF KO mice subjected to CLP only ( $277.3 \pm 123.2$  pg/mL vs  $37.2 \pm 35.8$  pg/mL;  $P = .0001$ ).

### HB-EGF KO mice have decreased survival after CLP

There was no mortality in HB-EGF KO mice or WT mice subjected to sham operation (Fig 6). WT mice subjected to CLP had significantly improved survival compared with HB-EGF KO mice subjected to CLP (9% [1/11] vs 0% [0/11];  $P = .0085$ ). None of the HB-EGF KO mice subjected to CLP survived  $>5$  days. Although no significance was noted between WT mice subjected to CLP but treated with HB-EGF and WT mice subjected to CLP only (18% [2/11] vs 9% [1/11];  $P = .4944$ ), HB-EGF KO mice subjected to CLP but treated with HB-EGF had increased survival compared with HB-EGF KO mice subjected to CLP only (18% [2/11] vs 0% [0/11];  $P = .0049$ ).

## DISCUSSION

The inherent capacity of epithelial cells to regenerate enables intestinal repair and healing even after extensive mucosal destruction. Loss of surface epithelium and villous structure is among the most important factors during intestinal injury. Animal models and clinical data support the concept that intestinal injury results in increased gut permeability with subsequent release of bacteria and endotoxin into the systemic circulation, which serves as the major inciting event leading to the systemic inflammatory response syndrome and subsequent multiple organ dysfunction syndrome.<sup>15,38,39</sup> Our current study shows that, compared with WT mice, deletion of the HB-EGF gene predisposes mice to peritonitis-

induced intestinal injury, with decreased villous length, increased intestinal permeability, increased IEC apoptosis, decreased inflammatory cytokine production, and decreased survival. We further show that administration of HB-EGF to WT and HB-EGF KO mice subjected to CLP increases villous length, improves gut barrier function, decreases IEC apoptosis, and decreases bacterial translocation. Furthermore, administration of HB-EGF to HB-EGF KO mice exposed to CLP improves survival. Taken together, these findings demonstrate the importance of HB-EGF in preserving gut barrier function after peritonitis-induced intestinal injury.

Previous studies from our laboratory have shown that HB-EGF plays an important role in maintaining intestinal barrier integrity in several models of intestinal injury. We have shown that HB-EGF KO mice exposed to experimental NEC have increased intestinal injury and increased intestinal permeability.<sup>28</sup> We have also shown that HB-EGF gene deletion is associated with intestinal barrier dysfunction in mice subjected to HS/R<sup>27</sup> and to superior mesenteric artery occlusion.<sup>26</sup> These results demonstrate that endogenous HB-EGF is important in intestinal barrier function. Because HB-EGF KO mice have deletion of HB-EGF only, with preservation of other EGF family members (data not shown), our current and previous results show that the effect of loss of HB-EGF on gut barrier function cannot be compensated for by the presence of other EGF family members.

Previous data from our laboratory demonstrate that administration of HB-EGF to rat pups exposed to experimental NEC or adult rats exposed to I/R significantly decreases enteric bacterial translocation to MLN.<sup>40,41</sup> Our current findings demonstrate that loss of endogenous HB-EGF expression increases the bacterial load in the PF and MLN after CLP, and that administration of HB-EGF can decrease the bacterial translocation observed. This is important, because there is a correlation between bacterial translocation and subsequent sepsis, which likely accounts for the survival advantage conferred to HB-EGF KO mice subjected to CLP but treated with HB-EGF.

Our current study indicates that 24 hours after CLP, HB-EGF KO mice have decreased pro- and anti-inflammatory cytokine levels. This suggests that loss of HB-EGF expression results in a poor response to inflammation caused by bacterial invasion. It is well known that a proper level of inflammation during infection is necessary and crucial for inhibiting bacterial growth and translocation after inflammation occurs.<sup>42</sup> We postulate that the poor response to bacteria-induced inflammation in the early stage of peritonitis leads to excessive bacterial growth and poor survival in HB-EGF KO mice subjected to CLP. In our model, administration of HB-EGF to HB-EGF KO mice subjected to CLP led to increased anti-inflammatory IL-10 levels in the serum, consistent with a partially restored response to bacteria-induced inflammation.

Using a model in which mice overexpress epidermal growth factor (EGF) in villi, Clark et al<sup>2</sup> demonstrated preservation of villus structure and length, decreased apoptosis in the intestine, and preservation of the intestinal proliferative response after CLP. In those studies, systemic administration of EGF conferred a survival advantage, but did not reduce the bacterial burden or cytokine levels in PF or blood.<sup>2</sup> In contrast, our studies show that HB-EGF administration results in decreased bacterial translocation and decreased pro-inflammatory cytokine levels after CLP. It has been shown that HB-EGF binds to and activates ErbB-1 to promote cell proliferation and chemotaxis, and also activates ErbB-4 to stimulate chemotaxis. Because HB-EGF binds to the EGF receptor (ErbB-1, EGFR) with a 10-fold greater affinity than EGF, it may act as a more potent mitogen and chemoattractant than EGF.<sup>17</sup> In addition, the ability of HB-EGF to bind to low-affinity, high-concentration cell-surface heparin sulfate proteoglycans may enhance its binding to EGFR.<sup>43</sup> The current observation that HB-EGF KO mice have lower survival after CLP compared with WT mice

highlights the importance of endogenous HB-EGF expression as an important survival factor in animals suffering from peritonitis.

In the current study, we utilized a model of sepsis based on CLP to examine the effects of HB-EGF administration. The CLP model is very different in pathophysiology compared with the I/R model<sup>31</sup> or the HS/R model<sup>24</sup> that we have used in our previous studies. The initiator of the CLP model is bacterial invasion, which causes endotoxemia and sepsis, whereas the model of I/R or HS/R is initiated by low local or systemic blood perfusion, which causes inflammation and oxidative damage to the intestines and other organs.<sup>44</sup> The CLP model is felt to be an ideal model for investigating bacterial peritonitis, as is commonly seen in the hospital setting, justifying our use of this model in the current studies.

Our results support an important protective role for HB-EGF in a model of sepsis based on CLP. Compared with WT mice, mice with loss of endogenous HB-EGF expression have significantly increased IEC apoptosis, pro-inflammatory cytokine expression, intestinal permeability, and mortality after CLP, which can be reversed with administration of exogenous HB-EGF. Administration of HB-EGF to WT mice subjected to CLP resulted in improved apoptosis indices and pro-inflammatory cytokine levels, although the results did not reach statistical significance. However, it is possible that examination at different time points after CLP may have resulted in significant results. Although WT mice subjected to CLP that were treated with HB-EGF had a 100% higher survival rate compared with WT mice subjected to CLP only (2/11 vs 1/11), the sample size of the survival study may have precluded significance of these results.

Taken together, our results demonstrate the ability of HB-EGF to confer a survival advantage and to improve intestinal barrier function in a murine model of sepsis. These findings support a role for HB-EGF as a novel preventive or therapeutic agent for the treatment of peritonitis-induced sepsis in the future.

## Acknowledgments

Supported by NIH R01 GM61193 (GEB).

The authors thank Dr. David Lee (Chapel Hill, NC) for supplying HB-EGF KO and WT mice, William Gardner, PhD and Wei Wang, MS, MAS, for their assistance with statistical analyses, and Claudio Lagoa, DVM, for assistance with establishing the CLP model.

## REFERENCES

1. Angus DC, Linde-Zwirble WT, Lidicker J, Clermont G, Carcillo J, Pinsky MR. Epidemiology of severe sepsis in the United States: analysis of incidence, outcome, and associated costs of care. *Crit Care Med.* 2001; 29:1303–1310. [PubMed: 11445675]
2. Clark JA, Gan H, Samocha AJ, Fox AC, Buchman TG, Coopersmith CM. Enterocyte-specific epidermal growth factor prevents barrier dysfunction and improves mortality in murine peritonitis. *Am J Physiol Gastrointest Liver Physiol.* 2009; 297:G471–G479. [PubMed: 19571236]
3. Clark JA, Coopersmith CM. Intestinal crosstalk: a new paradigm for understanding the gut as the “motor” of critical illness. *Shock.* 2007; 28:384–393. [PubMed: 17577136]
4. Hassoun HT, Kone BC, Mercer DW, Moody FG, Weisbrodt NW, Moore FA. Post-injury multiple organ failure: the role of the gut. *Shock.* 2001; 15:1–10. [PubMed: 11198350]
5. De-Souza DA, Greene LJ. Intestinal permeability and systemic infections in critically ill patients: effect of glutamine. *Crit Care Med.* 2005; 33:1125–1135. [PubMed: 15891348]
6. Neal MD, Leaphart C, Levy R, Prince J, Billiar TR, Watkins S, et al. Enterocyte TLR4 mediates phagocytosis and translocation of bacteria across the intestinal barrier. *J Immunol.* 2006; 176:3070–3079. [PubMed: 16493066]



7. Coopersmith CM, Stromberg PE, Dunne WM, Davis CG, Amiot DM II, Buchman TG, et al. Inhibition of intestinal epithelial apoptosis and survival in a murine model of pneumonia-induced sepsis. *JAMA*. 2002; 287:1716–1721. [PubMed: 11926897]
8. Hotchkiss RS, Swanson PE, Freeman BD, Tinsley KW, Cobb JP, Matuschak GM, et al. Apoptotic cell death in patients with sepsis, shock, and multiple organ dysfunction. *Crit Care Med*. 1999; 27:1230–1251. [PubMed: 10446814]
9. Osterberg J, Ljungdahl M, Haglund U. Influence of cyclooxygenase inhibitors on gut immune cell distribution and apoptosis rate in experimental sepsis. *Shock*. 2006; 25:147–154. [PubMed: 16525353]
10. Mainous MR, Ertel W, Chaudry IH, Deitch EA. The gut: a cytokine-generating organ in systemic inflammation? *Shock*. 1995; 4:193–199. [PubMed: 8574754]
11. Jiang J, Bahrami S, Leichtfried G, Redl H, Ohlinger W, Schlag G. Kinetics of endotoxin and tumor necrosis factor appearance in portal and systemic circulation after hemorrhagic shock in rats. *Ann Surg*. 1995; 221:100–106. [PubMed: 7826148]
12. Wang W, Smail N, Wang P, Chaudry IH. Increased gut permeability after hemorrhage is associated with upregulation of local and systemic IL-6. *J Surg Res*. 1998; 79:39–46. [PubMed: 9735238]
13. Calvano SE, Thompson WA, Marra MN, Coyle SM, de Riesthal HF, Trousdale RK, et al. Changes in polymorphonuclear leukocyte surface and plasma bactericidal/permeability-increasing protein and plasma lipopolysaccharide binding protein during endotoxemia or sepsis. *Arch Surg*. 1994; 129:220–226. [PubMed: 7508221]
14. Baker JW, Deitch EA, Li M, Berg RD, Specian RD. Hemorrhagic shock induces bacterial translocation from the gut. *J Trauma*. 1988; 28:896–906. [PubMed: 3294427]
15. Deitch EA. Multiple organ failure. Pathophysiology and potential future therapy. *Ann Surg*. 1992; 216:117–134. [PubMed: 1503516]
16. Besner G, Higashiyama S, Klagsbrun M. Isolation and characterization of a macrophage-derived heparin-binding growth factor. *Cell Regul*. 1990; 1:811–819. [PubMed: 2088527]
17. Higashiyama S, Abraham JA, Miller J, Fiddes JC, Klagsbrun M. A heparin-binding growth factor secreted by macrophage-like cells that is related to EGF. *Science*. 1991; 251:936–939. [PubMed: 1840698]
18. Bulus N, Barnard JA. Heparin binding epidermal growth factor-like growth factor is a transforming growth factor beta-regulated gene in intestinal epithelial cells. *Biochem Biophys Res Commun*. 1999; 264:808–812. [PubMed: 10544013]
19. Cribbs RK, Harding PA, Luquette MH, Besner GE. Endogenous production of heparin-binding EGF-like growth factor during murine partial-thickness burn wound healing. *J Burn Care Rehabil*. 2002; 23:116–125. [PubMed: 11882801]
20. Xia G, Martin AE, Besner GE. Heparin-binding EGF-like growth factor downregulates expression of adhesion molecules and infiltration of inflammatory cells after intestinal ischemia/reperfusion injury. *J Pediatr Surg*. 2003; 38:434–439. [PubMed: 12632363]
21. Jin K, Mao XO, Sun Y, Xie L, Jin L, Nishi E, et al. Heparinbinding epidermal growth factor-like growth factor: hypoxia-inducible expression in vitro and stimulation of neurogenesis in vitro and in vivo. *J Neurosci*. 2002; 22:5365–5373. [PubMed: 12097488]
22. Frank GD, Mifune M, Inagami T, Ohba M, Sasaki T, Higashiyama S, et al. Distinct mechanisms of receptor and nonreceptor tyrosine kinase activation by reactive oxygen species in vascular smooth muscle cells: role of metalloprotease and protein kinase C-delta. *Mol Cell Biol*. 2003; 23:1581–1589. [PubMed: 12588978]
23. McCarthy DW, Downing MT, Brigstock DR, Luquette MH, Brown KD, Abad MS, et al. Production of heparin-binding epidermal growth factor-like growth factor (HB-EGF) at sites of thermal injury in pediatric patients. *J Invest Dermatol*. 1996; 106:49–56. [PubMed: 8592081]
24. El-Assal ON, Radulescu A, Besner GE. Heparin-binding EGF-like growth factor preserves mesenteric microcirculatory blood flow and protects against intestinal injury in rats subjected to hemorrhagic shock and resuscitation. *Surgery*. 2007; 142:234–242. [PubMed: 17689691]

25. Feng J, El-Assal ON, Besner GE. Heparin-binding epidermal growth factor-like growth factor decreases the incidence of necrotizing enterocolitis in neonatal rats. *J Pediatr Surg.* 2006; 41:144–149. [PubMed: 16410124]
26. El-Assal ON, Paddock H, Marquez A, Besner GE. Heparin-binding epidermal growth factor-like growth factor gene disruption is associated with delayed intestinal restitution, impaired angiogenesis, and poor survival after intestinal ischemia in mice. *J Pediatr Surg.* 2008; 43:1182–1190. [PubMed: 18558204]
27. Zhang HY, Radulescu A, Besner GE. Heparin-binding epidermal growth factor-like growth factor is essential for preservation of gut barrier function after hemorrhagic shock and resuscitation in mice. *Surgery.* 2009; 146:334–339. [PubMed: 19628093]
28. Radulescu A, Yu X, Orvets ND, Chen Y, Zhang HY, Besner GE. Deletion of the heparin-binding epidermal growth factor-like growth factor gene increases susceptibility to necrotizing enterocolitis. *J Pediatr Surg.* 2010; 45:729–734. [PubMed: 20385279]
29. Zhang HY, Radulescu A, Chen CL, Olson JK, Darbyshire AK, Besner GE. Mice overexpressing the gene for heparin-binding epidermal growth factor-like growth factor (HBEGF) have increased resistance to hemorrhagic shock and resuscitation. *Surgery.* 2011; 149:276–283. [PubMed: 20965535]
30. Radulescu A, Zhang HY, Yu X, Olson JK, Darbyshire AK, Chen Y, et al. Heparin-binding epidermal growth factor-like growth factor overexpression in transgenic mice increases resistance to necrotizing enterocolitis. *J Pediatr Surg.* 2010; 45:1933–1939. [PubMed: 20920709]
31. El-Assal ON, Besner GE. HB-EGF enhances restitution after intestinal ischemia/reperfusion via PI3K/Akt and MEK/ERK1/2 activation. *Gastroenterology.* 2005; 129:609–625. [PubMed: 16083716]
32. Radulescu A, Zorko NA, Yu X, Besner GE. Preclinical neonatal rat studies of heparin-binding EGF-like growth factor in protection of the intestines from necrotizing enterocolitis. *Pediatr Res.* 2009; 65:437–442. [PubMed: 19127210]
33. Yu X, Radulescu A, Zorko N, Besner GE. Heparin-binding EGF-like growth factor increases intestinal microvascular blood flow in necrotizing enterocolitis. *Gastroenterology.* 2009; 137:221–230. [PubMed: 19361505]
34. James IA, Chen CL, Huang G, Zhang HY, Velten M, Besner GE. HB-EGF protects the lungs after intestinal ischemia/reperfusion injury. *J Surg Res.* 2010; 163:86–95. [PubMed: 20599214]
35. Jackson LF, Qiu TH, Sunnarborg SW, Chang A, Zhang C, Patterson C, et al. Defective valvulogenesis in HB-EGF and TACE-null mice is associated with aberrant BMP signaling. *EMBO J.* 2003; 22:2704–2716. [PubMed: 12773386]
36. Baker CC, Chaudry IH, Gaines HO, Baue AE. Evaluation of factors affecting mortality rate after sepsis in a murine cecal ligation and puncture model. *Surgery.* 1983; 94:331–335. [PubMed: 6879447]
37. Liaudet L, Soriano FG, Szabo E, Virag L, Mabley JG, Salzman AL, et al. Protection against hemorrhagic shock in mice genetically deficient in poly(ADP-ribose)polymerase. *Proc Natl Acad Sci U S A.* 2000; 97:10203–10208. [PubMed: 10954738]
38. Rotstein OD. Pathogenesis of multiple organ dysfunction syndrome: gut origin, protection, and decontamination. *Surg Infect (Larchmt).* 2000; 1:217–223. [PubMed: 12594892]
39. Fink MP, Delude RL. Epithelial barrier dysfunction: a unifying theme to explain the pathogenesis of multiple organ dysfunction at the cellular level. *Crit Care Clin.* 2005; 21:177–196. [PubMed: 15781156]
40. Feng J, Besner GE. Heparin-binding epidermal growth factor-like growth factor promotes enterocyte migration and proliferation in neonatal rats with necrotizing enterocolitis. *J Pediatr Surg.* 2007; 42:214–220. [PubMed: 17208569]
41. Xia G, Martin AE, Michalsky MP, Besner GE. Heparin-binding EGF-like growth factor preserves crypt cell proliferation and decreases bacterial translocation after intestinal ischemia/reperfusion injury. *J Pediatr Surg.* 2002; 37:1081–1087. [PubMed: 12077776]
42. Dinarello CA. Role of pro- and anti-inflammatory cytokines during inflammation: experimental and clinical findings. *J Biol Regul Homeost Agents.* 1997; 11:91–103. [PubMed: 9498158]

43. Higashiyama S, Abraham JA, Klagsbrun M. Heparin-binding EGF-like growth factor stimulation of smooth muscle cell migration: dependence on interactions with cell surface heparan sulfate. *J Cell Biol.* 1993; 122:933–940. [PubMed: 8349739]
44. Simms, HH. Models of adult respiratory syndrome - aspiration. In: Souba, WW.; Wilmore, DW., editors. *Surgical Research*. San Diego: Academic Press; 2001. p. 393-400.

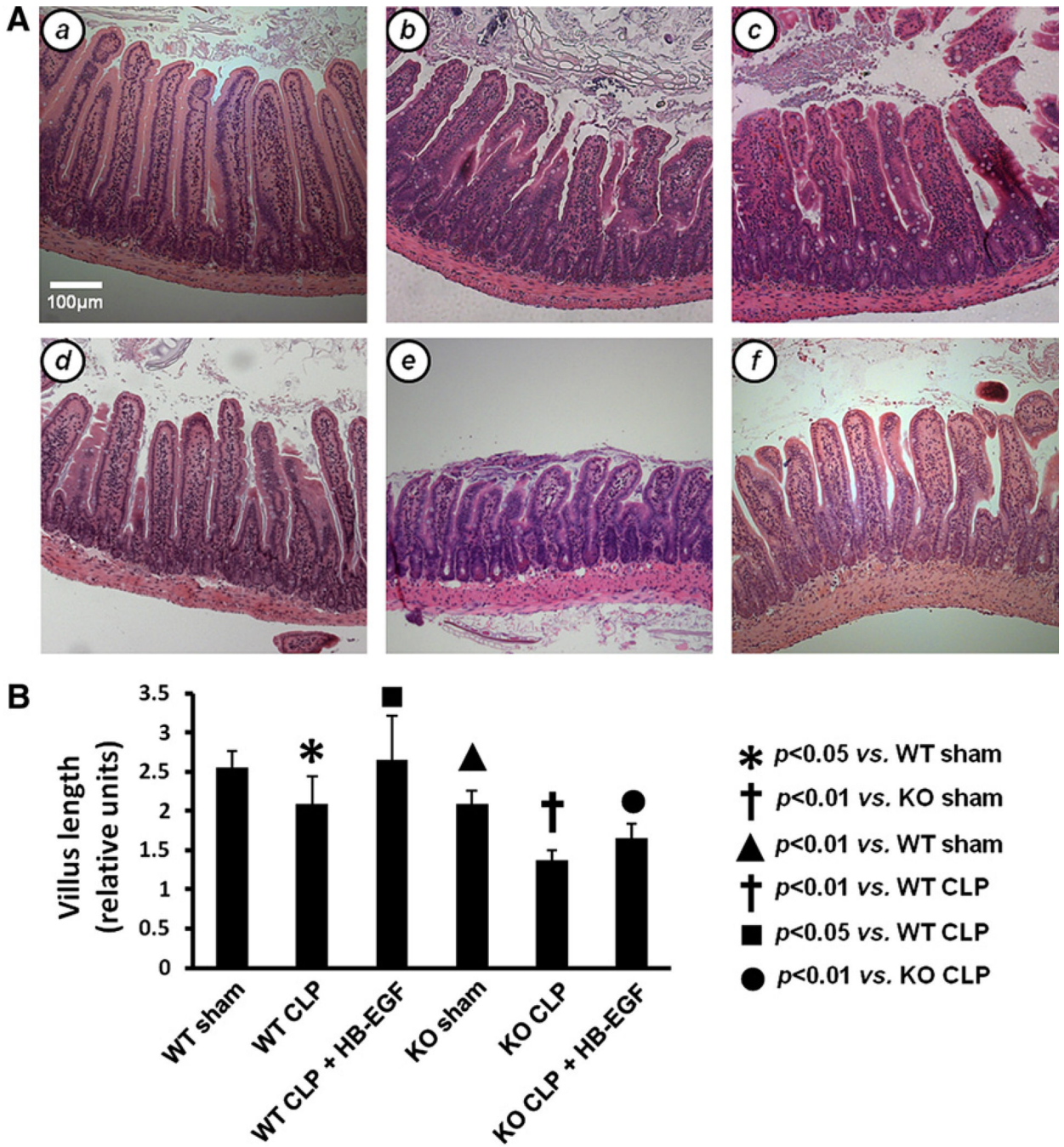


**Fig 1.** Intestinal villous length. *A*, Representative H&E-stained histologic images of sections of jejunum from (a) WT mice subjected to sham operation ( $n = 5$ ); (b) WT mice subjected to CLP ( $n = 4$ ); (c) WT mice subjected to CLP but treated with HB-EGF ( $n = 6$ ); (d) HB-EGF KO mice subjected to sham operation ( $n = 4$ ); (e) HB-EGF KO mice subjected to CLP ( $n = 5$ ); and (f) HB-EGF KO mice subjected to CLP but treated with HB-EGF ( $n = 5$ ). Original magnification,  $\times 100$ . *B*, Quantification of villous length. Villous length was measured as the distance from the crypt neck to the villous tip using Image J software. *KO*, HB-EGF KO mice; *WT*, wild type.

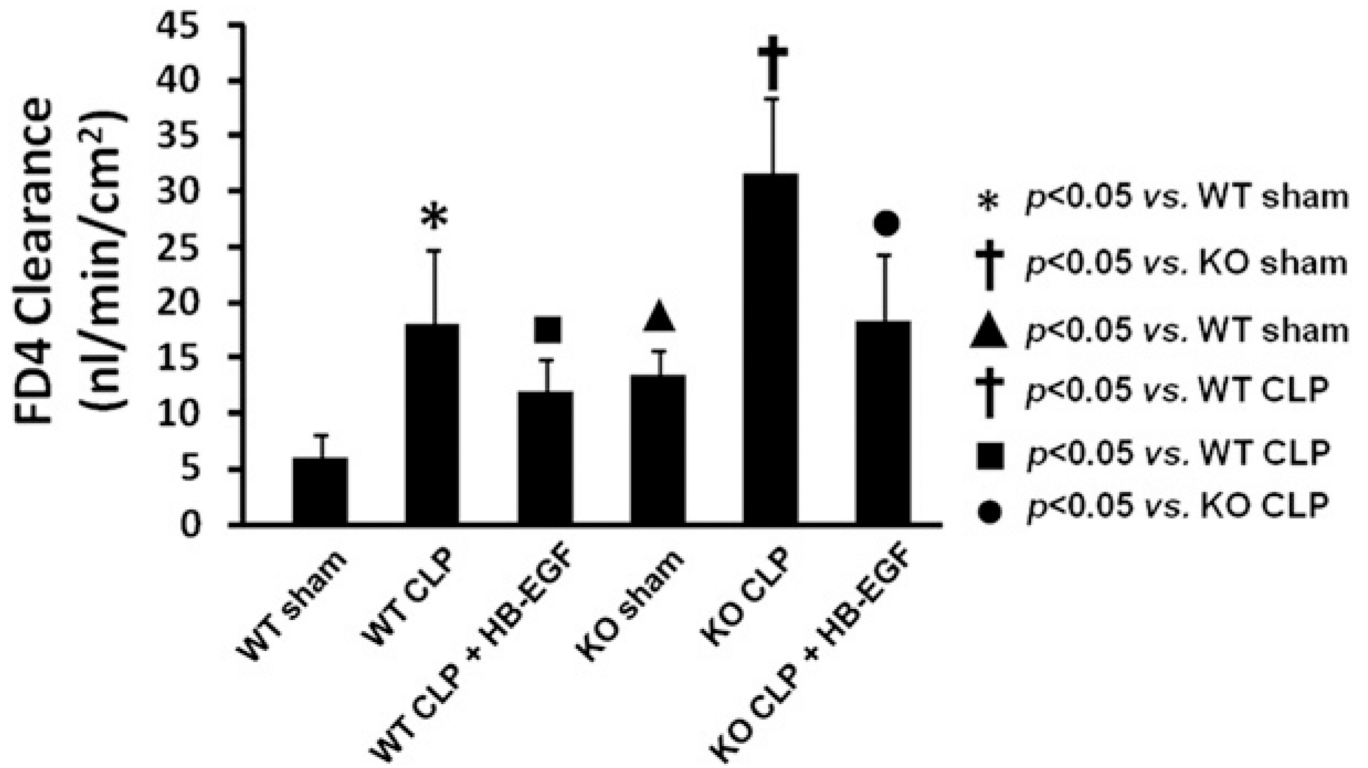


**Fig 2.** Intestinal permeability was determined by FD4 clearance in everted gut sacs in WT mice subjected to sham operation ( $n = 3$ ), WT mice subjected to CLP ( $n = 7$ ), WT mice subjected to CLP but treated with HB-EGF ( $n = 9$ ), HB-EGF KO mice subjected to sham operation ( $n = 2$ ), HB-EGF KO mice subjected to CLP ( $n = 5$ ), and HB-EGF KO mice subjected to CLP but treated with HB-EGF ( $n = 6$ ). *KO*, HB-EGF KO mice; *WT*, wild type.



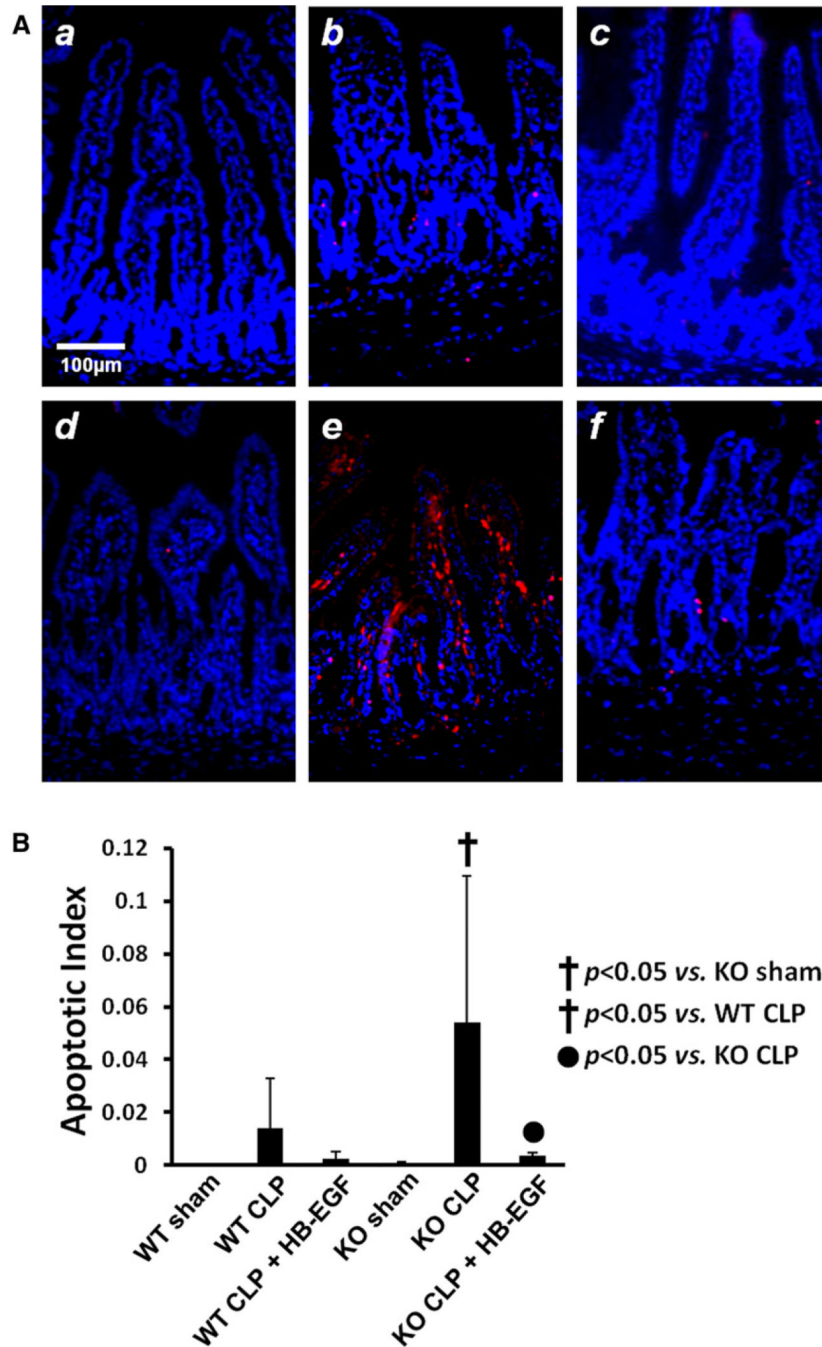


**Fig 3.**

**A**, Representative histologic images of sections of jejunum subjected to terminal deoxynucleotidyl transferase dUTP nick end labeling staining (*red*) and DAPI nuclear counterstaining (*blue*) from (*a*) WT mice subjected to sham operation ( $n = 5$ ); (*b*) WT mice subjected to CLP ( $n = 9$ ); (*c*) WT mice subjected to CLP but treated with HB-EGF ( $n = 7$ ); (*d*) HB-EGF KO mice subjected to sham operation ( $n = 4$ ); (*e*) HB-EGF KO mice subjected to CLP ( $n = 5$ ); (*f*) HB-EGF KO mice subjected to CLP but treated with HB-EGF ( $n = 5$ ). Original magnification,  $\times 200$ . **B**, Positively stained enterocytes and total enterocytes were counted using Image Pro Plus 6.2.1 for Windows, and the apoptotic index was defined as the

percent of positively stained enterocytes per 100 enterocytes. *KO*, HB-EGF KO mice; *WT*, wild type.

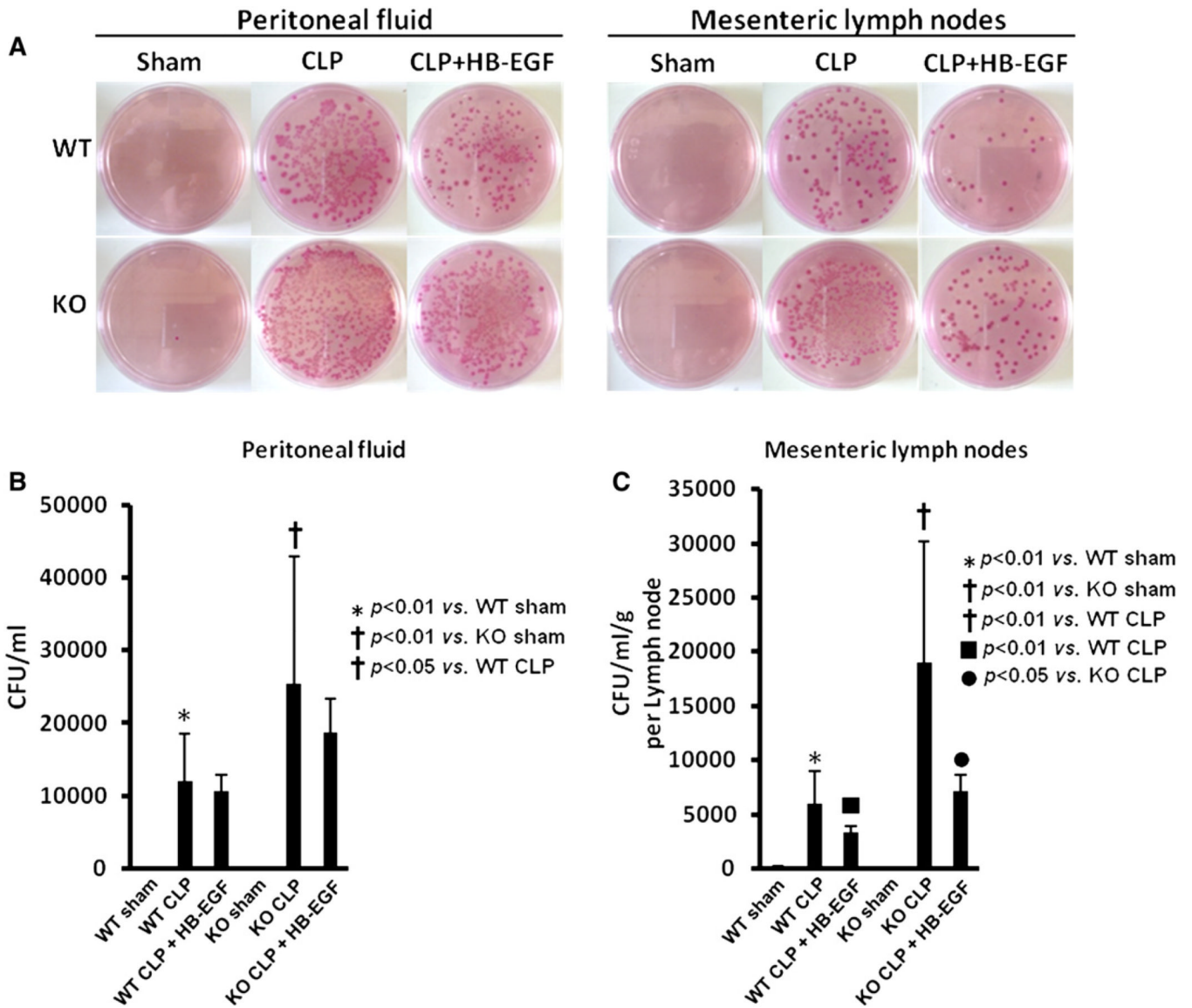


**Fig 4.** Bacterial growth in PF and mesenteric lymph nodes. *A*, Representative MacConkey agar plates demonstrating bacterial growth from the PF and mesenteric lymph nodes of WT mice subjected to sham operation ( $n = 2$ ), WT mice subjected to CLP ( $n = 5$ ), WT mice subjected to CLP but treated with HB-EGF ( $n = 6$ ), HB-EGF KO mice subjected to sham operation ( $n = 2$ ), HB-EGF KO mice subjected to CLP ( $n = 4$ ), and HB-EGF KO mice subjected to CLP but treated with HB-EGF ( $n = 6$ ). *B*, Quantification of bacterial colony forming units (CFU) in PF. *C*, Quantification of bacterial CFU in mesenteric lymph nodes. *KO*, HB-EGF KO mice; *WT*, wild type. (Color version of figure is available online.)

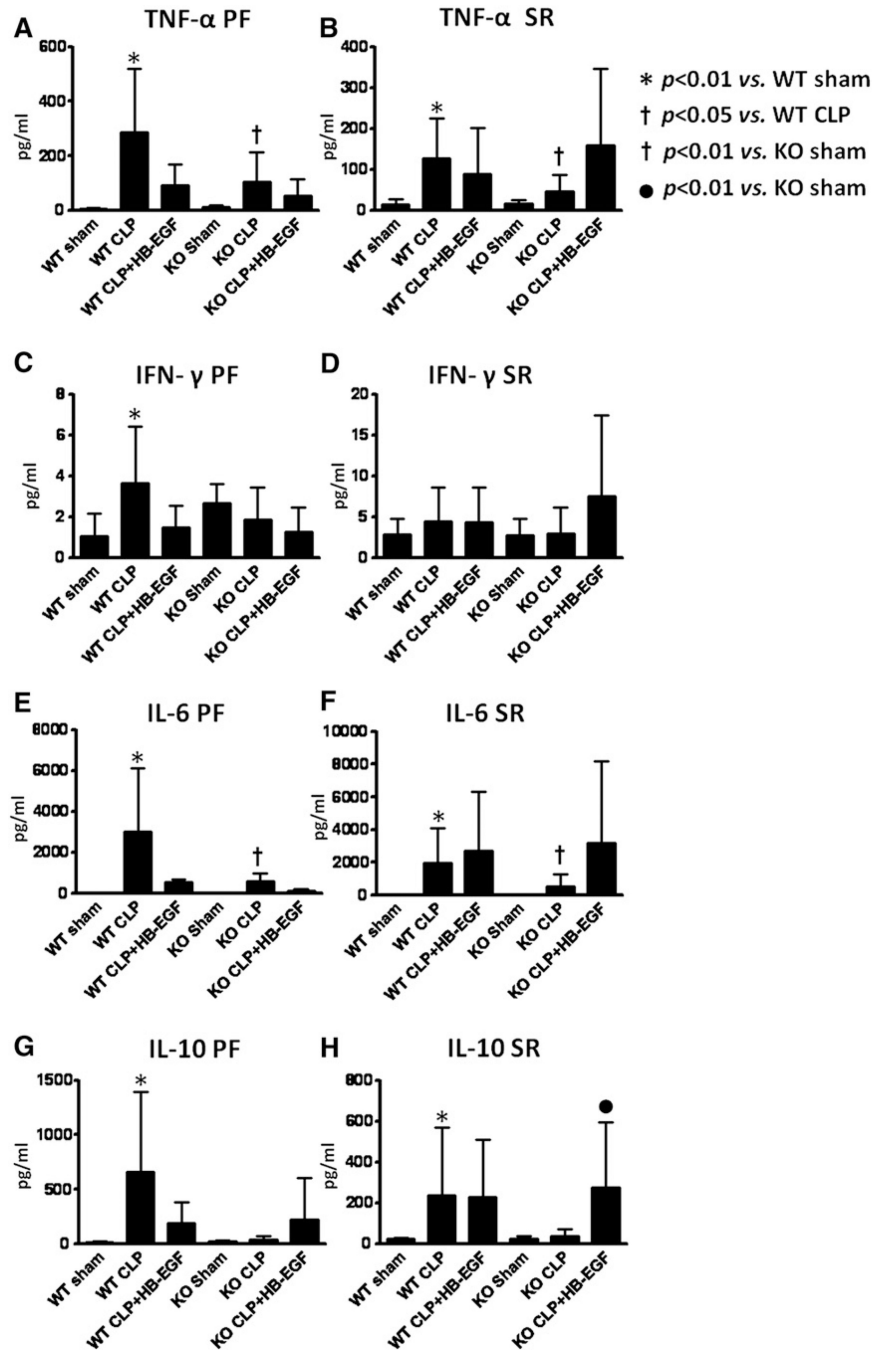


**Fig 5.** Pro- and anti-inflammatory cytokine levels were determined in peritoneal fluid (PF) and serum (SR) obtained 24 hours after surgery from WT mice subjected to sham operation ( $n = 9$ ), WT mice subjected to CLP ( $n = 14$ ), WT mice subjected to CLP but treated with HB-EGF ( $n = 10$ ), HB-EGF KO mice subjected to sham operation ( $n = 9$ ), HB-EGF KO mice subjected to CLP ( $n = 16$ ), and HB-EGF KO mice subjected to CLP but treated with HB-EGF ( $n = 6$ ). Data are expressed as mean values  $\pm$  SD.

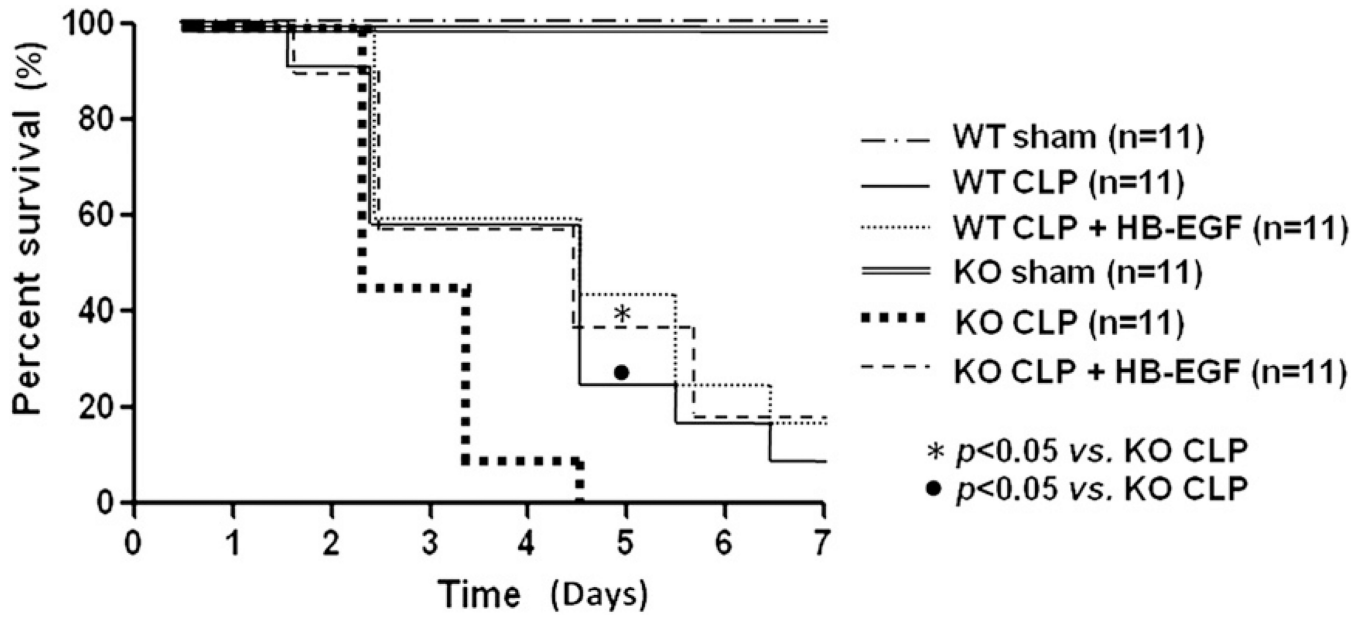


**Fig 6.** WT and HB-EGF KO mice were subjected to either sham operation or to CLP, with either HB-EGF or vehicle only administration. All mice were followed for survival for 7 days. *KO*, HB-EGF KO mice; *WT*, wild type.